Available online at www.sciencedirect.com
ScienceDirect
Ceramics International 35 (2009) 1219–1226
CERAMICS INTERNATIONAL
www.elsevier.com/locate/ceramint

High-density YSZ tapes fabricated via the multi-folding lamination process

X.G. Capdevila [a], J. Folch [b,*], A. Calleja [a], J. Llorens [a], M. Segarra [a], F. Espiell [a], J.R. Morante [b]

[a] *DIOPMA/CeRMAE, Departament d'Enginyeria Química i Metal·lúrgia, Facultat de Química, Universitat de Barcelona, Barcelona 08028, Catalonia, Spain*
[b] *EME/CeRMAE, Departament d'Electrònica, C/Marti i Franques, 1 (2a Planta), Facultat de Física, Universitat de Barcelona, Barcelona 08028, Catalonia, Spain*

Received 21 August 2007; received in revised form 22 September 2007; accepted 14 June 2008
Available online 5 August 2008

Abstract

A new method of ceramic processing to obtain high green and fully sintered yttria-stabilized zirconia (YSZ) ceramic parts has been studied. The procedure involved slip casting, multi-folding lamination, and sintering. A rheological study revealed correlation between compositional parameters and densities. A particular method of folding and lamination we named multi-folding lamination was proved to be an appropriate route to obtain dense, homogeneous green bodies, reaching density values of *ca.* 61%. Further studies on the sintered parts were performed in this work, obtaining YSZ sintered tapes suitable for the use in high temperature solid-state devices. This tapes, sintered at 1550 °C, reached values of 98% of theoretical density and average particle sizes within 1.7–12 μm.

Keywords: A: Tape casting; A: Sintering; E: Fuel Cells; YSZ

1. Introduction

High ionic conduction performances involve nearly full density ceramic structures with high chemical stability and mechanical toughness. Yttria-stabilized zirconia (YSZ) as oxygen ion conductor is widely selected to cover this goal, offering a broad range of technological possibilities in the fields of gas sensing and energy production. The typical example can be found in the automotive industry with the zirconia lambda probe [1,2]. According to literature, YSZ exhibits ionic conductivity at temperatures above 300 °C [3], and the high ionic conductivity needed for gas sensing devices is reached at temperatures around 500 °C [4], while fuel cells require temperatures in the range 800–1000 °C [5].

An accurate definition and control of the ceramic processing method establishes the properties of the resulting YSZ ceramic part. Comparatively to alternative techniques, colloidal processing is one of the most advantageous methods for the preparation of dense ceramic microstructures [6–8]. It may be divided in four basic steps: powder synthesis, suspension preparation, green body casting and drying, and solid-state sintering.

Related to powder synthesis, the doping level for a maximum ionic conductivity of YSZ is around 8 mol% yttrium oxide [9,10]. When using powders in the sub-micron particle size range, the control of colloidal processing through rheological measurement becomes a critical point [6,11–13]. Ceramics researchers have been conducting the formation of the pre-sintered body through proceeding with dry- [14–16] and wet-forming techniques [13,17–18], all of them being reliant on the intended purposes: high density, appropriate mechanical strength, flexibility, and/or good machinability [7,19]. Particularly, wet-forming techniques offer a high degree of simplicity and suitability for developing ceramic parts with complex shape [6].

Solid-state sintering process produces coalescence among neighboring ceramic particles, increasing grain size and reducing the overall porosity [20]. At a technological level,

* Corresponding author. Tel.: +34 93 403 91 54; fax: +34 93 402 11 48.
E-mail address: jfolch@el.ub.es (J. Folch).

0272-8842/$34.00
doi:10.1016/j.ceramint.2008.06.018

the sintering profile (namely, temperature gradients over time and isothermal holding time) defines the final microstructure [21].

The aim of this work was to study the relation between the processing techniques, specially multiple lamination and the main structural properties of the YSZ green and sintered bodies.

2. Experimental

2.1. Materials

The microstructural features of the purchased YSZ (8 mol% yttrium oxide) powder (Tosoh Corp., Japan) were crystallite size 56 nm, primary particle size 0.35 μm, spherical secondary aggregate size of 20 μm, and a specific surface area of 5.8 m^2/g (BET N_2 adsorption method). The calculated theoretical density (TD), obtained from published data (82-1244. JCPDS-International Centre for Diffraction Data) was 5.953 g/cm^3. X-ray diffraction showed a single cubic phase in those powders.

The ceramic slurries were based on a solvent system produced with azeotropic mixtures of ethanol (99.8%; Panreac, Spain) and toluene (>99.5%; Riedel-deHaën, Germany) for the rheological measurements, and ethanol with *p*-xylene (>99%; Fluka, Germany) for the casting process.

The selected dispersing agent was a low molecular weight alkyl phosphate ester ('Surtech 421'; Surface Chemists of Florida, USA). The tested binders were ethylcellulose (Fluka, Germany), and polyvinyl butyral (PVB) ('Butvar B98'; Solutia, USA).

The plastisizing function was performed through a composition based on dibutyl phthalate (DBP) (>98%; Fluka, Germany) and polyethylene glycol (PEG-400; Merck, Germany).

Firstly, we performed preliminary tests combining the previously listed components, for the obtainment of a starting slurry with homogeneous composition and suitable to be tested under the subsequent evaluation techniques and rheological measurement.

2.2. Optimization of dispersing agent concentration

The initially performed procedure was a rheological study of the colloidal system in order to adjust dispersant concentration. The viscosimeter consisted of a controlled stress rheometer (HAAKE RS100, Germany) with a parallel plate sensor (20 mm in diameter and 0.4 mm of gap). The colloidal suspensions were prepared by mixing the YSZ powder, the solvent and the additive mixtures, followed by ultrasonication (Ultrasonic Bandelin Sonoplus, Germany) for 5 min. Creep tests were conducted to get zero shear viscosity, η_0. It was found that stationary regimes were not completely reachable, indicating that samples were slightly time-dependent. Therefore, a time of 300 s was prescribed to determine a comparative zero shear rate viscosity, which was minimized as a function of dispersing agent concentration. Fig. 1 shows a typical viscosity versus dispersing agent concentration plot.

From these graphs we selected the additive concentration for the minimum viscosity of the slurry [8,13].

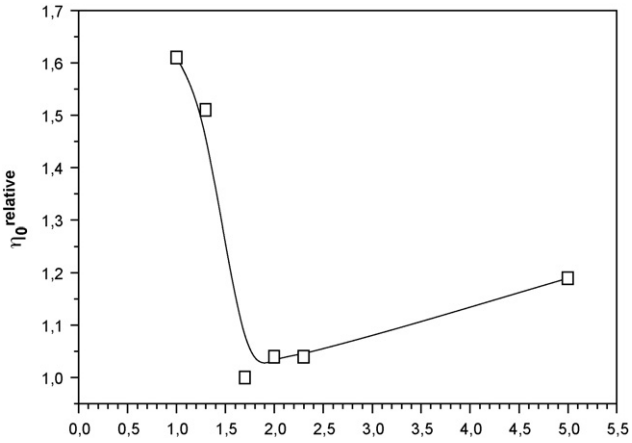

Fig. 1. Viscosity of the slurry versus dispersing agent concentration. The values of η_0 obtained during the tests were expressed as relative values compared to the minimum.

2.3. Slip preparation and casting

The ceramic slurry was prepared by following a two-step process, as suggested by Mistler and Twiname [6], in which the compositional adjustment of binder, plasticizer, and solids loading was performed. In the first step, the YSZ powder was introduced into a zirconia ball-mill jar, containing a solvent and a dispersant, and processed in a Pulverisette 300 ball-milling machine for 24 h. This stage breaks down the soft-agglomerates between YSZ particles, distributes the powder particles as homogeneously as possible, and suspends the ceramic particles for the following processing step. In the second step, the binder and the plasticizers were poured into the milling jar, and mixed for additional 24 h to homogeneously surround the deflocculated YSZ particles.

The resulting paste was deposited and squeezed in a cylindrical stainless steel mould, composed of a die with a removable perimetral ring. The slurry was dried in air at 22 °C and a relative humidity of 70%. During that process the green tape lost a great percentage of the solvents and acquired its characteristic properties of flexibility and surface smoothness.

2.4. Multi-folding lamination of the casted green body

The tape is removed from the mould after a drying time of 3 days. In this work we proposed a novel lamination method focused on both improving particle packaging and ensuring tape homogeneity. The lamination process consisted in a combination of lamination, bending and rotation. Fig. 2 illustrates the proposed multi-folding lamination process. Each stage consists in four laminating and bending steps, and a sample rotation of 90° in the lamination plane. The lamination steps were performed maintaining constant the gap between two stainless steel rollers. We also studied the effect of the number of bending steps and the lamination thickness. The selected number of stages was between zero and four. At the same time, lamination thicknesses of 0.55, 0.65, and 0.75 mm were tested.

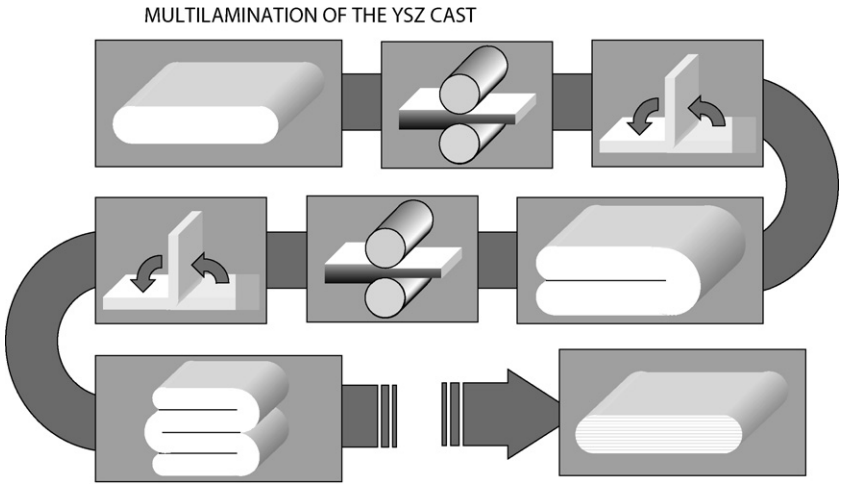

Fig. 2. Sequence of the proposed multi-lamination process. Each stage consists in four laminating and bending steps, followed by a rotation of 90° parallel to the lamination plane.

2.5. Sintering profile

The sintering profiles were performed in a tube furnace (Eurotherm, UK). The heating rates, soak times and peak temperatures were optimized in order to (1) avoid any warpage at high temperature removing the remaining solvent, (2) submit the organic components (PEG, DBP, PVB) to an complete pyrolysis, and (3) to fully densify the final ceramic part in the sintering process. Table 1 summarizes the main features for different sintering schedules. To evaluate the evolution of density and grain size versus sintering temperature and identify the stages of solid-state sintering, several samples were sintered at 1400, 1450, 1500 and 1550 °C. The effect of the soak time at maximum temperature was also tested. The selected times were 10 min and 1, 2, 6, and 10 h.

After the drying step, the sintering profile included an organics burn-out dwell. The organics were totally removed by soaking 2 h at 500 °C. According to reported thermo-gravimetric analysis, most of PVB char is considered to be eliminated at temperatures of about 350–450 °C [22].

The measurement of fired densities was made by Archimedes method, using isopropyl alcohol as the immersion media. Numerical values were referenced to theoretical density.

In order to determine the grain sizes, cross-sections and surfaces of the densified ceramics were polished using 1 μm diamond paste, then thermally etched at 1300 °C for 30 min to reveal grain boundaries. Assuming the particles were spheres, the estimated true grain sizes can be calculated by multiplying the apparent grain sizes, determined from SEM micrographs, by a factor of 1.57, using a software-assisted linear intercept method.

3. Results and discussion

3.1. Optimal concentration of organic components

The used YSZ powder has been shown to have agglomerates loose enough to break down under the milling process [23]. As Gibson et al., pointed out the predominance of soft agglomerates in the initial powder is a required factor for a proper particle compaction in the green ceramics [16].

The dispersing agent, a low molecular weight alkyl phosphate ester, adsorbs at the solid–liquid interface and infers a repulsive force between the ceramic particles, which keeps the particles well dispersed. Steric interaction, due to the

Table 1
Matrix of tested sintering conditions

Function	Schedule	Results
Solvents evaporation	100 °C/2 h	Good
Burn-out ramp	0.5 °C/min	Good
	1 °C/min	Warpage. Detrimental to densification
Burn-out isotherm	450 °C/2 h	Warpage. Detrimental to densification
	500 °C/2 h	Good
Pre-sintering	800 °C	Detrimental to densification
Sintering ramp	1 °C/min	Good
	2 °C/min	Detrimental to densification
	3 °C/min	Detrimental to densification
	4 °C/min	Detrimental to densification
Sintering isotherms	1400 °C	Low density: small grain size
	10 min	
	2 h	
	6 h	
	10 h	
	1450 °C	
	2 h	
	1500 °C	High density: grain size increasing with temperature and time
	10 min	
	1 h	
	2 h	
	6 h	
	10 h	
	1550 °C	
	10 min	
	1 h	
	2 h	
	6 h	
	10 h	

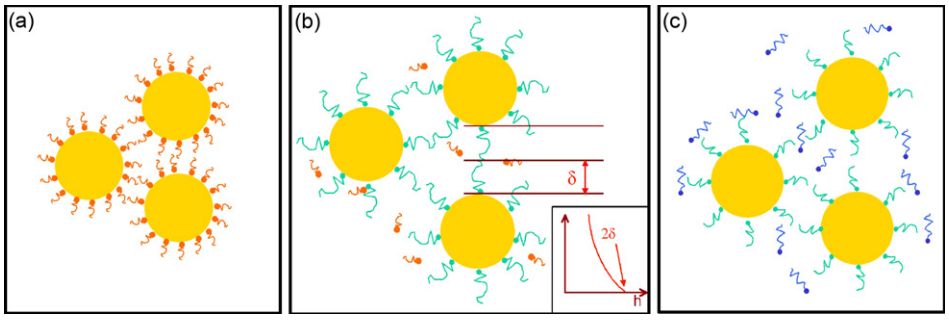

Fig. 3. (a) Alkyl phosphate esters ($R–O–PO_3H^-$) adsorb at the solid–liquid interface and infer a repulsive force between the ceramic particles, which keeps the particles well dispersed in the deagglomeration of ceramic particles during milling, (b) the binder gradually removes and substitutes the dispersant from the particles surface, while maintaining the deffloculation function and (c) platicizer shortens the binder tails.

alkyl chains, and electrical interactions, due to the phosphate group, take place simultaneously (Fig. 3(a)). These interactions act as barriers when the particles approach distances at which the attraction due to van der Waals forces could become effective.

After rheological adjustment, the ceramic slurry had a solid content of 59.2% (w/w) and a viscosity of 10 Pa s, with a concentration of dispersing agent of 1.7% (w/w) over dry basis. The measure was carried out under a shear stress (τ) of 7 Pa. This value was below the critic shear (τ_c) and we can assume that viscosity was independent of τ. The applied shear rate ($\dot{\gamma}$) was $1.4 \times 10^{-3}\ s^{-1}$.

The fundamental concern for dimensional stability and strength of the ceramic green body is faced through the introduction of a mixture of binders and plasticizers [24]. The binder covered those requirements while retaining the green body shape without affecting the final density. We found that an excess of binder negatively affects both density and sintered homogeneity, while a reduced amount results in an insufficient cohesion between ceramic particles during wet processing. The PVB binder gradually removed and substituted the dispersant from the particles surface, while maintaining the deffloculation function (Fig. 3(b)). In our case, we found that the optimum concentration of binder (PVB) was 10% (w/w) over dry basis.

The effect of the plasticizers (DBP and PEG) was to break the hydrogen bonds between YSZ particles and vinyl alcohol groups in PVB, which reduce the flexibility of the green ceramic material [24,25]. The binder conferred structure to the cast body, although it made the ceramic slurry excessively viscous, as well as excessive stiffness to the green body. To avoid these negative effects, plasticizers were added, which shortened the PVB tails formed by hydroxyl groups (Fig. 3(c)). This thinned the slurry and improved the flexibility of the resulting green body. In our case, we found that the optimum concentrations of plasticizers were 2.8% (w/w) of DBP and 3.7% (w/w) of PEG in dry basis.

3.2. The multi-folding lamination process

In principle, pressure enables a higher particle packing density [6,26]. Nevertheless, the multi-folding lamination process requires a trade-off between pressure and packing homogeneity. Additionally, the multi-folding lamination process improves surface homogeneity and smoothness. The gap between rollers was adjusted to avoid disruptive effects such as anisotropic densities or cracking produced when the pressure in the vertical (pressing) axis gave place to an expansion in the perpendicular plane [27]. Qualitatively, we observed that an excessive compression caused a warpage during the sintering process due to the introduced internal strains and inhomogeneities, which lead to uneven shrinkage and densification during the sintering process. The final optimal thickness was about 30% of the initial. At the same time, the vertical stresses were reduced. The multi-folding lamination shifted the green density value to *ca.* 61% TD (compare with densities about 50% obtained without use of multi-lamination steps). An example of the resulting sheet can be seen in Fig. 4. To the best of our knowledge, no published data involving similar methods has shown such high green density, as shown in Table 2.

3.3. Sintering profile evaluation

The features of the designed heating schedule can be grouped in the following parts: (a) pyrolysis temperature slope,

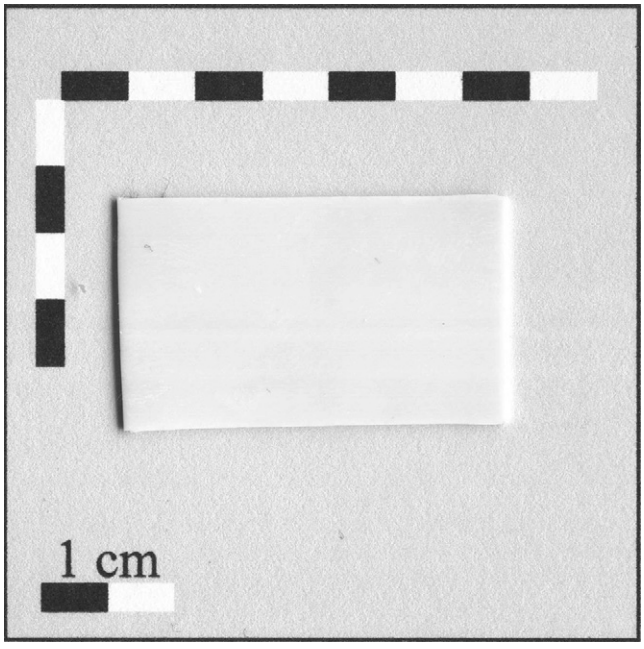

Fig. 4. Image of a typical sample of a fired YSZ sheet.

Table 2
Bibliographical survey of the methods and results for the production of green and fired YSZ bodies

Powder features	Green density (% TD)	Production method	Sintered density (% TD)	Sintering isotherm (°C, h)	Authors
Micron-size YSZ-8M	57	Tape casting	96.0	Conventional (1500, 4)	Mukherjee et al. [13]
Micron-size YSZ-8M	n.a.	Vacuum casting	98.1	Conventional (1600, 2)	He et al. [17]
Micron-size YSZ-8M	52	Uniaxial pressing	96.0	(1400, 2)	Leng et al. [14]
Micron-size YSZ-8M	54	Tape casting	96.0	(1550, 2)	Maiti and Rajender [8]
Micron-size YSZ-3M	n.a.	Injection moulding	99.7	(1500, 2)	Trunec et al. [28]
Micron-size YSZ-8M	n.a.	Isostatic pressing	99.3	(1500, 4)	Ciacchi et al. [15]
Micron-size YSZ-8M	45	Isostatic pressing	99.7	(1500, 2)	Gibson et al. [16]
Micron-size YSZ-8M	n.a.	Extrusion	n.a.	(1500, 2)	Du et al. [18]

(b) pyrolysis temperature, (c) pre-sintering introduction, and (d) sintering temperature and sintering dwell time. In Table 1 are summarized the global results for the designed process.

Regarding the burn-out ramp, we verified the adverse effects of the faster heating rates (see Table 1). The decomposition of each organic component overlapped in time, causing a too fast elimination of combustion gases, which produced bubbles, cracks, warpage and internal stresses, thus diminishing the final density.

The burn-out performed at temperatures lower than 500 °C did not eliminate completely the PVB molecules before the sintering ramp, impairing the quality of the resulting ceramic, with similar effects as too fast burn-out ramp. The selected burn-out soak time was 2 h.

A pre-sintering soak at 800 °C was investigated in order to test more efficient burn-out conditions. This step was found to be not useful to improve ceramic particles arrangement for the further process of sintering.

The sintering ramp yielding the highest densities was 1 °C/min. Faster ramps negatively affected the resulting densities. Rahaman attributed this detrimental effect to differential densification produced by transient stresses between ceramic particles during sintering [29].

3.4. Effect of sintering on particle diameter and density

We observed that the sintering soak parameters (temperature and time) affecting to different degrees the micro- and macrostructural features of the resulting solid YSZ electrolytes. From the obtained results the firing temperature has been found to be the main factor to determine the fired densities. We found that a temperature of 1400 °C is clearly insufficient to reach acceptably high densities, and low enough porosities. Moreover, grain growth was small, and grain size hardly attained a diameter around 1 μm (Fig. 5).

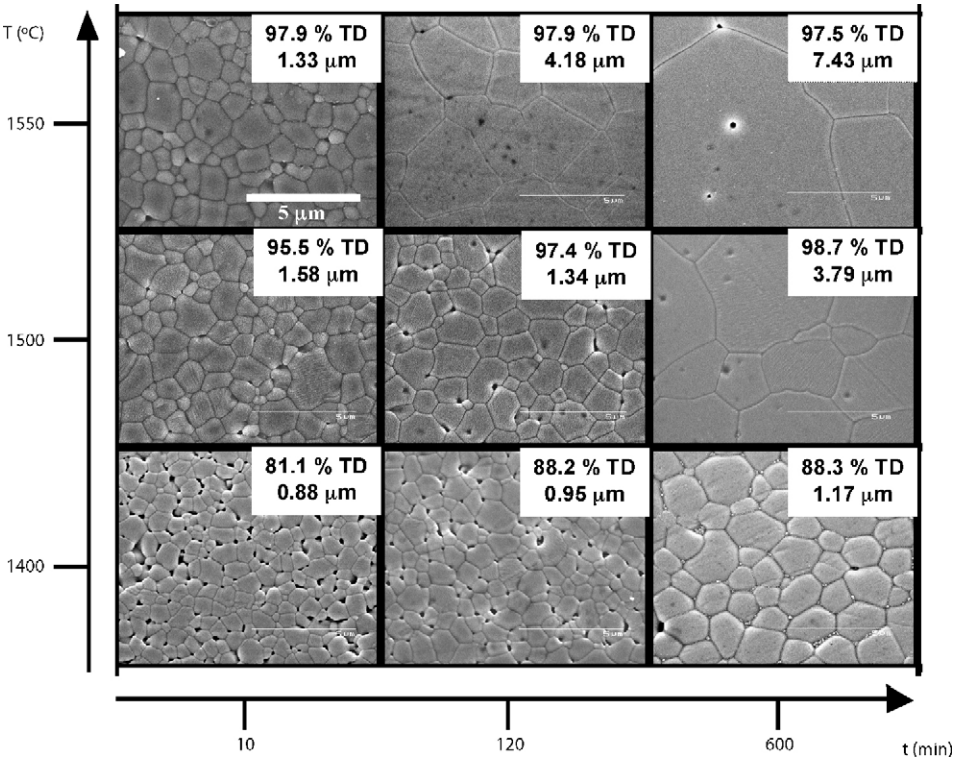

Fig. 5. SEM micrographs of YSZ sintered under different soak times and temperatures.

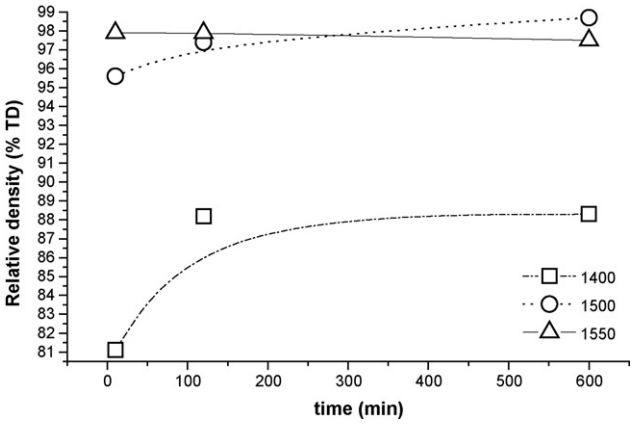

Fig. 6. Relative density versus dwell time at different temperatures.

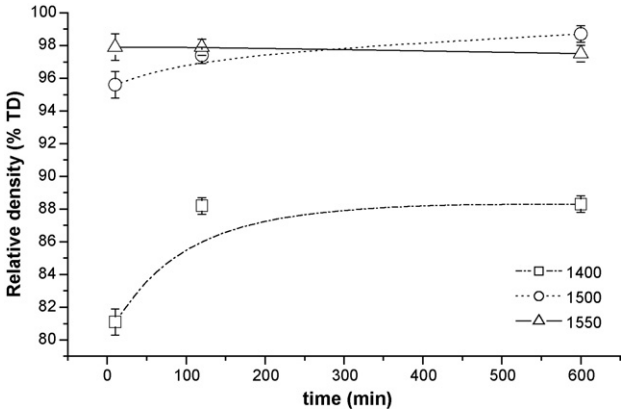

Fig. 7. Grain size versus dwell time at different temperatures.

Maximum densities and significantly greater particle sizes were obtained when sintering the samples at the temperatures of 1500 and 1550 °C, with the isothermal holding time being the defining factor of the resulting features. In these samples pore elimination was nearly completed, even when with the shortest firing time of 10 min, which resulted in the lowest density. These results are in agreement with theoretical models, which predict that pore shrinkage and grain growth are intrinsically related [30].

Density is mainly dependent on sintering temperature, however the effect of firing dwell time on the resulting features cannot be neglected. Essentially, the effect of holding time is twofold, and both the density and grain size after firing are affected. Related to the evolution of density under a fixed

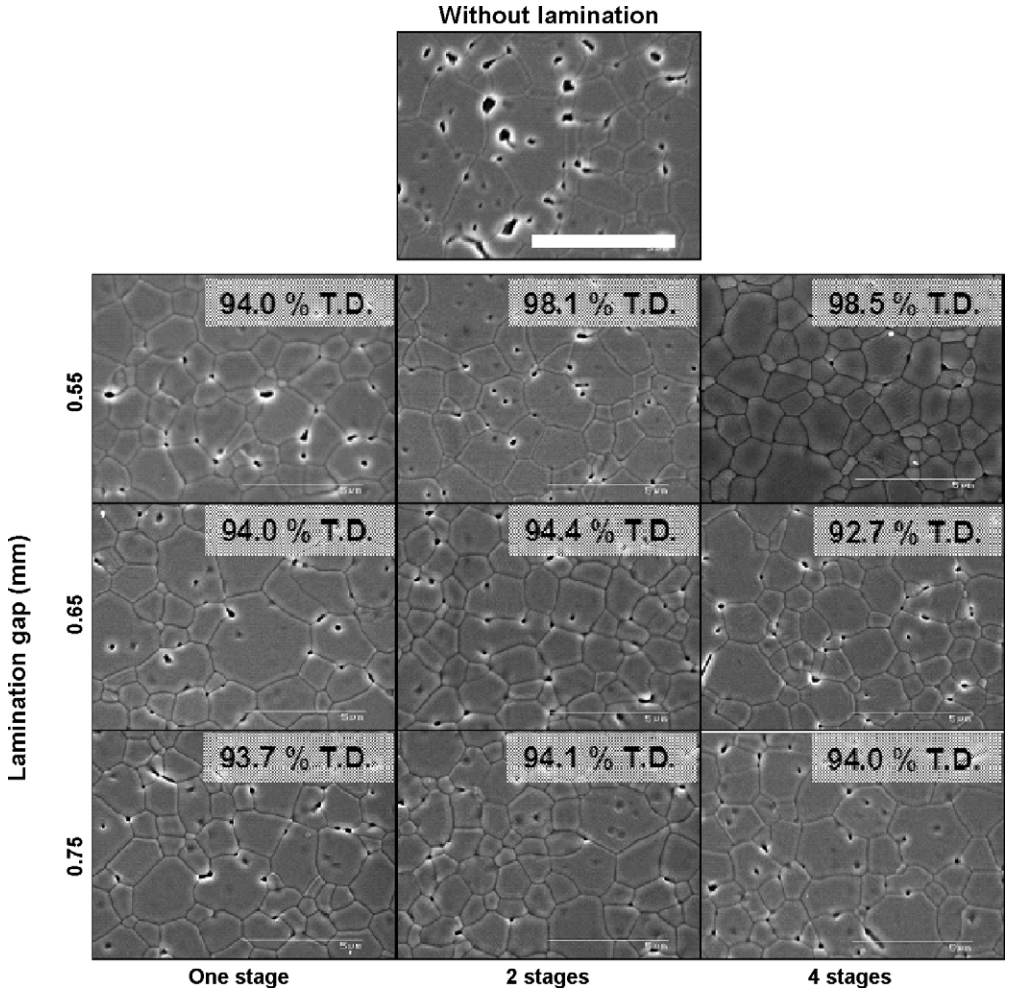

Fig. 8. Microstructure and fired density for samples submitted to different multi-lamination steps. The scale is the same for all the pictures.

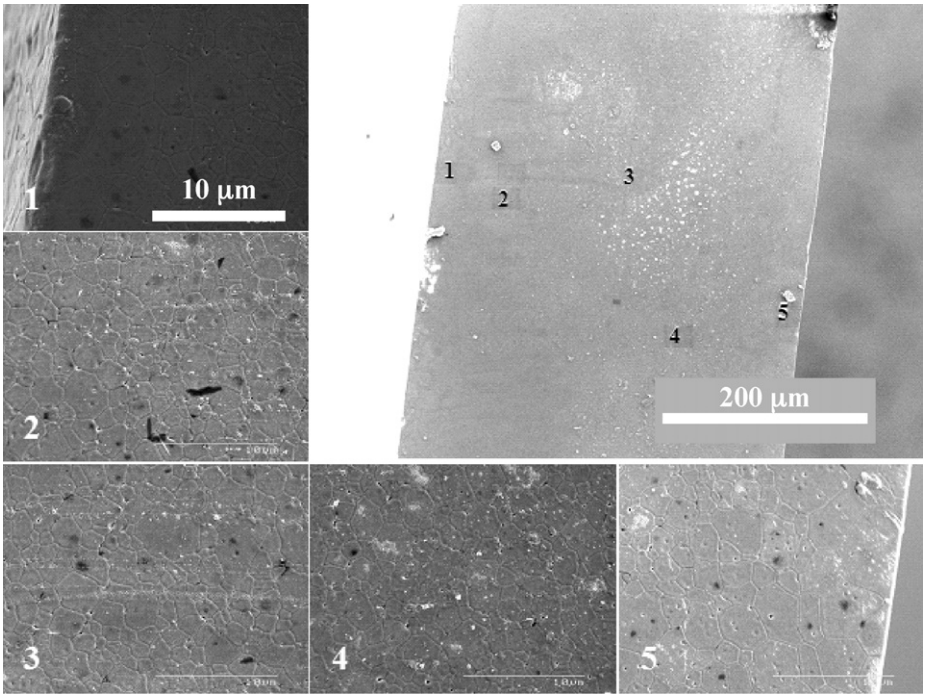

Fig. 9. Series of SEM cross-section micrographs for a sample submitted to multi-lamination with four rotation stages and sintering at 1550 °C for 2 h.

temperature, an increment in dwell time results in greater densification, reaching maximum density asymptotically (Fig. 6). As expected, the higher the firing temperature, the higher the resulting density. Nevertheless, for temperatures above 1500 °C, holding the sample for longer times cause a decrease of density. At these temperatures, grain coarsening rate becomes too high leading to abnormal grain growth with pores trapped inside large grains [29].

Grain size is mostly affected by isothermal holding time at temperatures over 1500 °C, providing enough energy for the activation of the grain growth process, as shown in Fig. 7. In this case, grain size can be adjusted to an exponential growth according to the following empirical equation [21]:

$$d = (d_0^n + k(t - t_0))^{1/n}$$

where d is the average grain size at time t, d_0 is the average grain size at time t_0, k is a temperature-dependent rate parameter and n is the exponent depending on the kinetics of the growth process which can be assumed an integer ranging from 1 to 4. Particularly,

$$k = A \exp\left(-\frac{E_a}{RT}\right)$$

where A is a constant, R is the gas constant, T is the absolute temperature, and E_a is the activation energy for grain growth. By adjusting this function to our data at an isothermal time of 10 h, we obtain an apparent value of 284 kJ/mol for E_a. This result is in accordance with literature values [10].

3.5. Effect of the lamination parameters over microstructure

According to Fig. 8, all samples displayed lower porosity than the one without lamination, which also had larger pore size. The lamination thickness had no significant effect on final density or porosity (see Fig. 8). Changing the number of lamination stages the pore size and morphology of the samples was slightly modified, generating the roundest and smallest pores for the sample with four lamination stages. With these results we found that the multi-lamination processes with thicknesses higher than 0.55 mm and involving less than four stages did not reach fully densified samples.

Cross-sections of a full density sample exhibited homogeneous grain size, excepting a 3-μm thick layer at both surfaces, which showed larger grain sizes (see Fig. 9). We attributed this effect to preferential atomic migration and consequently grain coarsening at the surface respect to bulk diffusion.

From a structural point of view, the obtained solid electrolytes YSZ are fine and can provide excellent electrical performances. We developed electrical testing to check the electrical performances of these YSZ electrolytes, to be analyzed in further studies.

4. Conclusions

The proposed multi-folding lamination process allows the control of inhomogeneities and the attainment of samples with higher green and sintered densities compared to using a tape casting process. Additionally, this method supports standard

ceramic low cost procedures and utilities, thus being available to industry.

By controlling the firing time and temperature parameters it is feasible to tailor the grain growth and fired density. The best fired densities were obtained for the samples sintered at 1500 °C for 6 h, and at 1550 °C for 2 h.

Acknowledgement

This work was performed under the auspices of CeRMAE, a scientific organization of the Government of Catalonia to provide funding for research in advanced materials and environment-friendly technologies.

References

[1] U. Adler, Electronic Gasoline Fuel-Injection System with Lambda Closed-Loop Control, L-Jetronic: Technical Instruction, Robert Bosch GmbH, 1985, ISBN 1-85-226008-4. http://www.digest.net/alfa/archive/v8/msg01828.html (August, 2002).

[2] J. Riegel, H. Neumann, H.-M. Wiedenmann, Exhaust gas sensors for automotive emission control, Solid State Ionics 152–153 (2002) 783–800.

[3] N. Docquier, S. Candel, Combustion control and sensors: a review, Prog. Energy Combust. Sci. 28 (2002) 107–150.

[4] K. Saji, H. Kondo, T. Takeuchi, I. Igarashi, Voltage step characteristics of oxygen concentration cell sensors for nonequilibrium gas mixtures, J. Electrochem. Soc. 135 (7) (1988) 1686–1691.

[5] T.A. Ramanarayanan, S.C. Singhal, E.D. Wachsman, High temperature ion conducting ceramics, interface, J. Electrochem. Soc. (2001).

[6] R.E. Mistler, E. Twiname, Tape Casting: Theory and Practice, The American Ceramic Society, Westerville, OH, USA, 2000.

[7] A. Roosen, H.K. Bowen, Influence of various consolidation techniques on the green microstructure and sintering behavior of alumina powders, J. Am. Ceram. Soc. 71 (11) (1988) 970–977.

[8] A.K. Maiti, B. Rajender, Terpineol as a dispersant for tape casting yttria stabilized zirconia powder, Mater. Sci. Eng. A 333 (2002) 35–40.

[9] I.R. Gibson, G.P. Dransfeld, J.T.S. Irvine, Influence of yttria concentration upon electrical properties and susceptibility to ageing of yttria-stabilised zirconias, J. Eur. Ceram. Soc. 18 (1998) 661–667.

[10] J. Nowotny, M. Rekas, T. Bak, Defect chemistry and defect-dependent properties of undoped and stabilised zirconia. bulk vs interface, in: E. Kisi (Ed.), Zirconia Engineering Ceramics, Trans Tech Publications Ltd., Switzerland, 1998, p. 223.

[11] J.A. Lewis, Colloidal processing of ceramics, J. Am. Ceram. Soc. 83 (10) (2000) 2341–2359.

[12] D.-M. Liu, Adsorption, rheology, packing, and sintering of nanosize ceramic powders, Ceram. Int. 25 (1999) 107–113.

[13] A. Mukherjee, B. Maiti, A. Das Sharma, R.N. Basu, H.S. Maiti, Correlation between slurry rheology, green density and sintered density of tape cast yttria stabilised zirconia, Ceram. Int. 27 (2001) 731–739.

[14] Y.-J. Leng, S.-H. Chan, K.-A. Khor, S.-P. Jiang, P. Cheang, Effect of characteristics of Y_2O_3/ZrO_2 powders on fabrication of anode-supported solid oxide fuel cells, J. Power Sources 117 (2003) 26–34.

[15] F.T. Ciacchi, K.M. Crane, S.P.S. Badwal, Evaluation of commercial zirconia powders for solid oxide fuel cells, Solid State Ionics 73 (1994) 49–61.

[16] I.R. Gibson, G.P. Dransfeld, J.T.S. Irvine, Sinterability of commercial 8 mol% yttria-stabilized zirconia powders and the effect of sintered density on the ionic conductivity, J. Mater. Sci. 33 (17) (1998) 4297–4305.

[17] T. He, Z. Lu, Y. Huang, P. Guan, J. Liu, W. Su, Characterization of YSZ electrolyte membrane tubes prepared by a vacuum casting method, J. Alloys Compd. 337 (2002) 23–236.

[18] Y. Du, N.M. Sammes, G.A. Tompsett, Optimisation parameters for the extrusion of thin YSZ tubes for SOFC electrolytes, J. Eur. Ceram. Soc. 20 (2000) 959–965.

[19] A. Roosen, Low-temperature/low-pressure lamination of green ceramic tapes, Adv. Eng. Mater. 2 (6) (2000) 374–376.

[20] J.L. Shi, Relation between coarsening and densification in solid-state sintering of ceramics: experimental test on superfine zirconia powder compacts, J. Mater. Res. 14 (4) (1999) 1389–1397.

[21] J.-G. Li, T. Ikegami, T. Mori, Low temperature processing of dense samarium-doped CeO_2 ceramics: sintering and grain growth behaviors, Acta Mater. 52 (2004) 2221–2228.

[22] L.A. Salam, R.D. Matthews, H. Robertson, Pyrolisis of polyvinyl butyral (PVB) binder in thermoelectric green tapes, J. Eur. Ceram. Soc. 20 (2000) 1375–1383.

[23] N.H. Menzler, D. Lavergnat, F. Tietz, E. Sominski, E. Djurado, W. Fischer, G. Pang, A. Gedanken, H.P. Buchkremer, Materials synthesis and characterization of 8YSZ nanomaterials for the fabrication of electrolyte membranes in solid oxide fuel cells, Ceram. Int. 29 (2003) 619–628.

[24] J.A. Lewis, K.A. Blackman, A.L. Ogden, Rheological property and stress development during drying of tape-cast ceramic layers, J. Am. Ceram. Soc. 79 (12) (1996) 3225–3234.

[25] K.-Y. Lim, D.H. Kim, U. Park, S.H. Kim, Effect of the molecular weight of poly(ethylene glycol) on the plasticization of green sheets composed of ultrafine $BaTiO_3$ particles and poly(vinyl butyral), Mater. Res. Bull. 38 (2003) 1021–1032.

[26] T.L. Wen, D. Wang, M. Chen, H. Tu, Z. Lu, Z. Zhang, H. Nie, W. Huang, Material research for planar SOFC stack, Solid State Ionics 148 (2002) 513–519.

[27] J.-S. Sung, K.-D. Koo, J.-H. Park, Lamination and sintering shrinkage behavior in multilayered ceramics, J. Am. Ceram. Soc. 82 (3) (1999) 537–544.

[28] M. Trunec, P. Dobšák, J. Cihlář, Effect of powder treatment on injection moulded zirconia ceramics, J. Eur. Ceram. Soc. 20 (2000) 859–866.

[29] M.N. Rahaman (Ed.), Ceramic Processing and Sintering, Marcel Dekker Inc., New York, 1995.

[30] S. Sibakumar, S. Subbanna, S.S. Sahay, V. Ramakrishnan, P.C. Kapur, Pradip, S.G. Malghan, Population balance model for solid state sintering. II. Grain growth, Ceram. Int. 27 (2001) 63–71.